10.1071/PVv2010n149p17

Study and application of the multiple small-aperture TEM system

Guo Wen Bo

Xue Guoqjang

W. B. Guo[1], G. Q. Xue[2,4], X. Li[3], H. J. Quan[3] and N. N. Zhou[2]

[1]*School of Electronic & Information Engineering, Xi'an Jiaotong University, Xi'an, China*
[2]*Key Laboratory of Mineral Resource, Institute of Geology & Geophysics, Chinese Academy of Sciences, Beijing, China*
[3]*College of Geology, Engineering & Geomatics, Chang'an University, Xi'an, China*
[4]*Corresponding author. Email: qqxueguoqiang@hotmail.com*

Nowadays the transient electromagnetic method (TEM) is widely used in ground surface exploration, due to its ease of operation, high precision, large information and sensitivity to low resistance bodies. In the last two years, TEM has begun to be used in underground studies to detect water filled structures ahead of the tunnel. Because of the excellent resolution of low resistance bodies and the secondary field responses directly received by the antenna, TEM has a bright future in tunnel prediction. During a tunnel survey, the scale length of the survey field is so small that it is not possible to lay a large enough loop. Redesigning the optimal survey configuration of TEM is important for improving the detection precision of TEM soundings. In this paper, we introduce a TEM array with multi-aperture survey configuration in which a large aperture single transmitter loop was substituted with several relatively small aperture TEM arrays. Then we study the primary and secondary TEM fields to find a coherent multi-source TEM field. Furthermore, a coherent stack of multiple transmitter sources can improve the intensities of the primary and secondary field. It is shown that the multiple small-aperture TEM system can improve the secondary field response by nearly 31%. A tunnel forecasting TEM system has been developed and a case study shows that it is an effective and successful method for exploring and predicting unfavorable geological structures ahead of the tunnel wall during tunnel drilling.

Keywords: TEM, tunnel, small-aperture, prediction

Introduction

In many parts of the world, fast economic development requires the construction of railways, highways, dams, hydroelectric facilities, as well as mining exploration to identify new resource deposits. Such activities frequently require drilling of extended tunnels through mountain regions with complex geological environments, which in turn introduces potentially dangerous problems, such as water or mud jetting and cave-ins. Consequently, practical geological prediction ahead of drilling is an important and necessary process during tunnel construction. One approach to this problem is to use geophysical prediction methods.

At present in China, to avoid any unnecessary harm to workers and economic losses, the Railway Bureau has decided to make the application of tunnel prediction technologies a routine procedure; similarly the Highway Department is beginning to pay more attention to tunnel forecasting. Based on the above observations, the development of advanced tunnel prediction technologies is an important issue for the future.

Normally, geophysical prediction methods include tunnel seismic prediction (TSP) (Dickmann and Sander, 1996), especially using seismic reflection tomography (SRT) and ground penetrating radar (GPR). This approach is not very sensitive to unfavourable geological bodies, especially when faults, caves and zones of rock fracture are filled with water or mud.

Several popular TEM transmitter-receiver configurations, including long off-set TEM (LOTEM – Spies and Parker, 1984; Strack et al., 1990), coincident loop (Raiche et al., 1985), large loop (Xue et al., 2004), and surface-borehole (Christensen and Sørensen, 1998; Zhang and Xiao, 2000), have been successfully applied in the areas of engineering exploration, mineral investigation and theoretical study. Multi-transmitter electromagnetic surveys (Zhdanov and Tartaras, 2002; Zhdanov, 2006) are widely used in remote-sensing and geophysical exploration. Multi-transmitter multi-receiver surveys have been investigated in the case of marine exploration. However, there are few reports on the study of multi-aperture TEM configurations.

After a modelling test, we developed a special TEM survey configuration, including four small transmitter loops and a receiver antenna. We used this system to measure the field response of a target body. After measuring a decay curve of secondary field voltage corresponding to a survey point, we moved the system to the next survey point until all measurements were recorded. Finally we obtained the data from a tunnel wall, then processed the data and interpreted the results. The case study has indicated that this technique can successfully detect water or mud-filled faults or fracture zones ahead of the front wall of a tunnel during construction.

Laboratory tests of the multi-aperture system

In order to test whether a multi-aperture source produces a larger primary and secondary field response, a conductive copper plate (32 cm × 24 cm × 2 mm) using a single and a multi-aperture transmitter configuration was excited, and the primary and secondary field responses were measured in terms of magnitude and alignment.

The single large-loop transmitter source consists of a square loop (20 cm × 20 cm with 10 turns); while the multi-aperture array consists of four smaller square loops (10 cm × 10 cm with 10 turns each) (see Figure 1). In each small-aperture transmitter source, the current direction was clockwise with a magnitude of 10 A. The transmitting power was 12 V and 50 soundings were stacked with a 25 Hz transmitting frequency during the primary and secondary field survey. The measurements were made on a square receiver loop (10 cm × 10 cm with 10 turns). The field is measured along the diagonal direction in the horizontal plane using a roaming receiver loop at different vertical displacements relative to the transmitter. In Figure 1*a* the current excited in each small-aperture loop is clockwise, so that the corresponding magnetic field is always in the same direction, which is equal to the single-aperture transmitter.

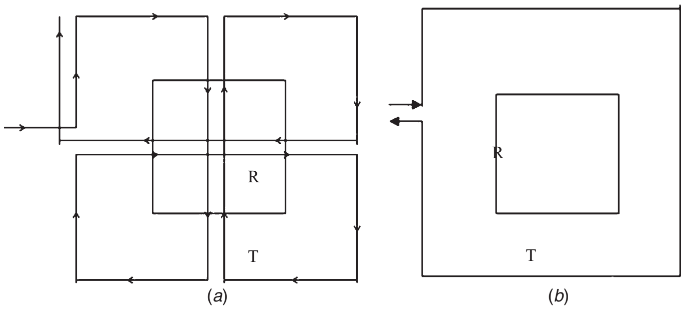

Fig. 1. *Multi-aperture transmitter configuration (a) a special transmitter configuration formed by four small loops; (b) a larger square loop configuration.*

Figure 2 shows the secondary field curves of the single (or standard) and the multi-aperture source without conductance model, where the vertical distance is 6 cm (Figure 2*a*), 8 cm (Figure 2*b*) and 10 cm (Figure 2*c*). From Figure 2 it is clear that the two curves almost agree with a small discrepancy when the conductance plate is non-existing. So we can ignore the difference of self-transients between the two configurations.

The purpose of measuring the primary field is to identify and characterise coherent properties of the multi-aperture field. We generated the primary fields through both the single large-aperture loop and the multiple small-aperture transmitter loops, and measured its strength as a function of horizontal position.

Figures 3*a* and 3*b* show the primary field contour maps, at 6 cm vertical distance relative to the transmitter, excited by the single large-loop source and by the multiple small-aperture array source. In Figure 3*b* it is obvious that in the case of the multiple small-aperture array configuration, the primary field value at the centre is smaller than along the diagonal lines. The maximum value occurs approximately near the centre of the individual loops that make up the multi-aperture antenna. While in the case of the single large-aperture configuration, the primary field value (64.2 mV/a) in the centre of the loop is smaller than that of the value (7.2 mV/A) in the centre of the loop generated by

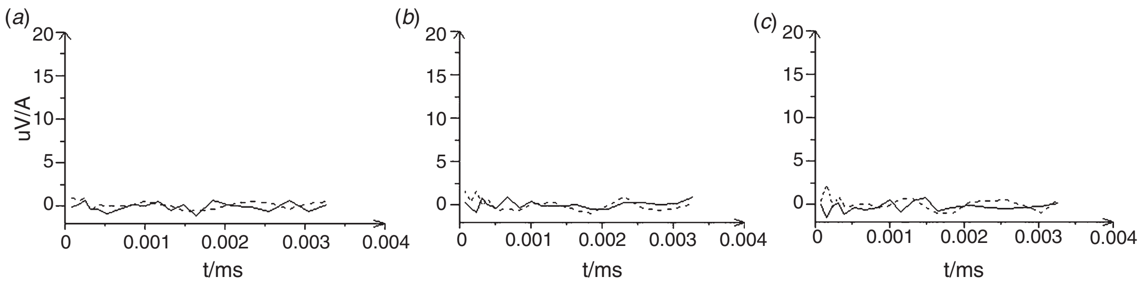

Fig. 2. *Secondary field curves of standard and multi-aperture source without conductance plate. Solid lines represent results with the standard source and dashed lines represent results with the multi-aperture source.*

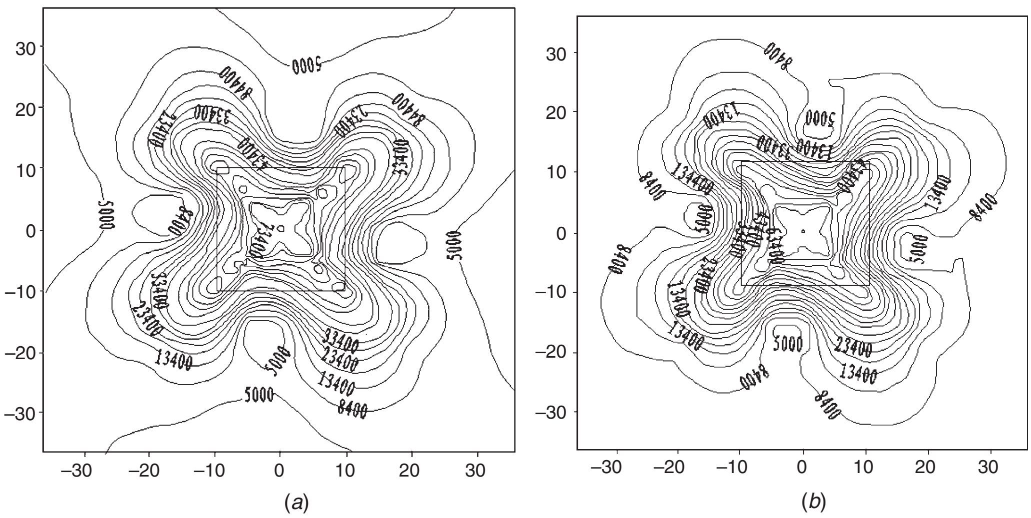

Fig. 3. *Multi-aperture (a) and single-loop (b) primary field contours at a vertical distance of 6 cm from the transmitter. The location of the transmitter loop is illustrated by a square.*

the multiple small-aperture arrays. The latter is approximately 10.9% larger than that of the former.

Figure 4 shows the curves of the field strengths with varied survey points under two different configurations. These results demonstrate that multiple small-aperture sources can generate a more powerful primary magnetic field. Furthermore, the multiple small-aperture transmitter configuration can create a coherent single primary field just as the single large-aperture transmitter configuration does.

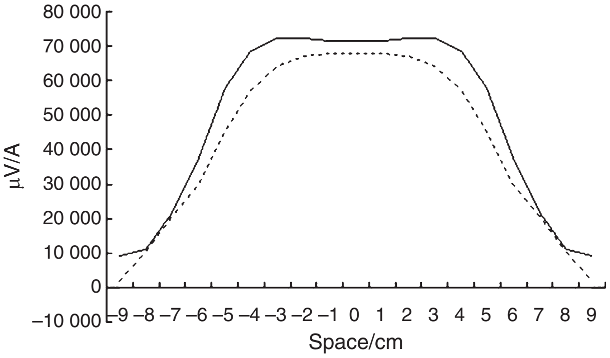

Fig. 4. *Multi-aperture and single-aperture primary field curve for different survey points at a vertical distance of 6 cm from the transmitter. Solid lines represent the primary field with a standard source and dashed lines represent the primary field with a multi-aperture source.*

The purpose of measuring the secondary field is to quantify the improved ability of the multiple small-aperture array sources to detect a low resistivity body compared to the single large-aperture source. We employed a copper plate (32 cm × 24 cm × 2 mm) to simulate a low resistivity body. We used the single large-loop and the multiple small-aperture transmitter sources to initiate electrical currents in the copper-plate at buried depths between 0 cm and 16 cm with 2 cm intervals. The results are shown in Figure 5. The transmitting power was 12 V, the transmitting frequency was 25 Hz and the current was 10 A. The time delay after switching off the two configurations was 0.087 ms, and the survey time range was from 0.087 ms to 7.19 ms.

Figure 5 illustrates that for the same buried depth, the response from the multiple small-aperture transmitter system is greater than that of the single large-aperture transmitter system. When the buried depth is increased from 0 cm to 6 cm the response

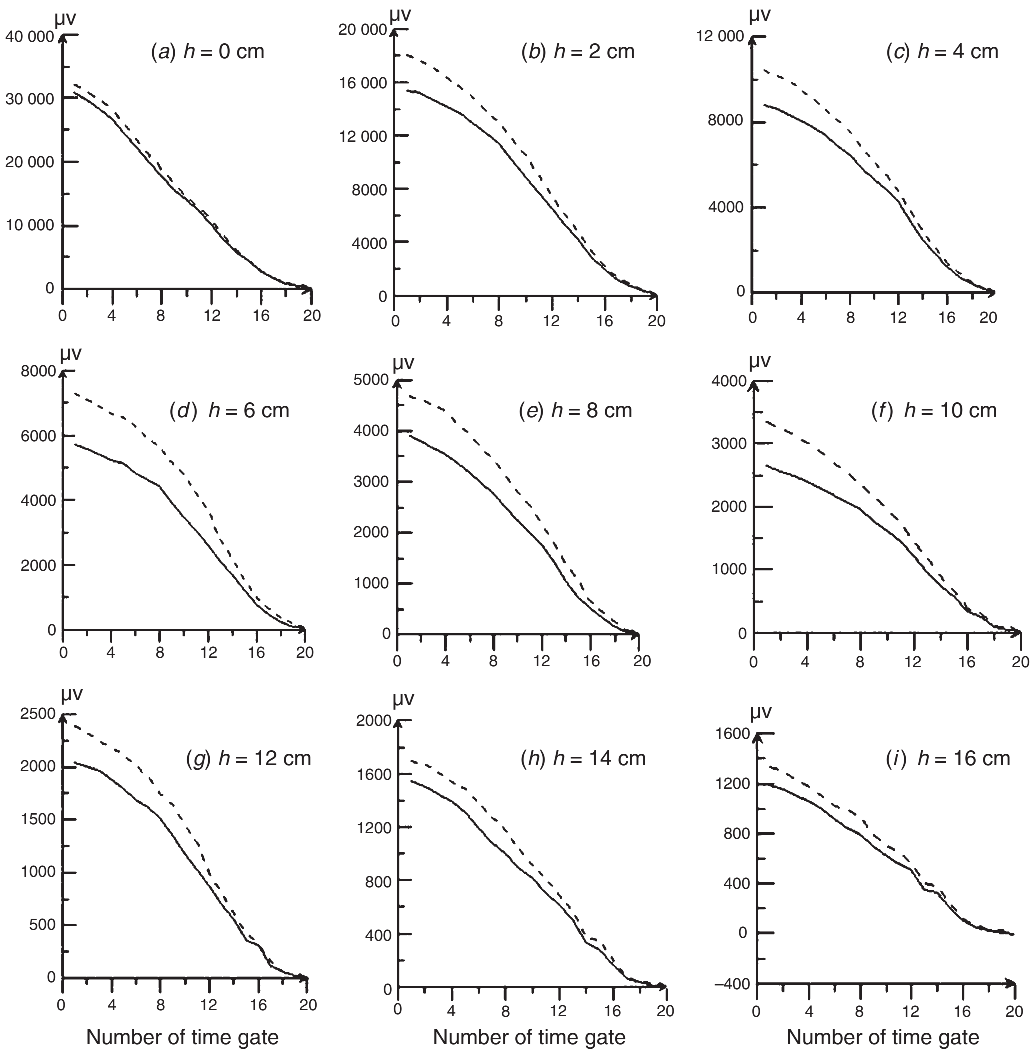

Fig. 5. *Secondary field voltage decay curves for conducting copper plate at different buried depths ranging from 0 cm to 16 cm. The dashed line represents the multi-aperture system response and the solid line represents the single aperture system response.*

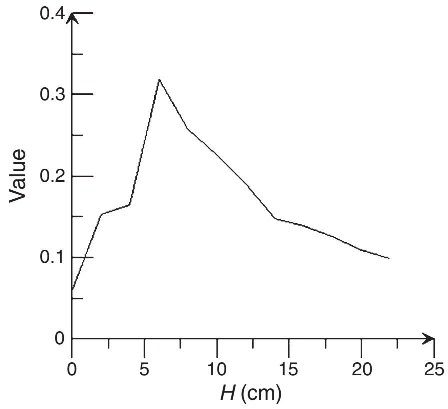

Fig. 6. *Curve of relative difference value between multi-aperture loop and single-aperture loop response to a conductive copper plate at various buried depths.*

difference between the two systems is increased becoming the largest at a depth of 6 cm (Figure 5*a*–*d*); hereafter the response difference decreases with buried depth from 6 cm to 16 cm.

In order to quantify the relationship between the copper plate response of the multiple small-aperture loops and the single large-aperture loop, we calculate the relative difference, defined as $(V_m - V_s)/V_s$, where V_m and V_s are the voltage for the multiple small-aperture loops and for the single large-aperture loop, respectively. The above relative values for the two systems with varied buried depths are shown in Figure 6, confirming the former conclusion that the largest value was observed at a buried depth of 6 cm, and from that buried depth the relative values decreased both in positive (from 6 cm to 22 cm) or negative (from 6 cm to 0 cm) directions.

We have demonstrated that the magnetic field generalised by the multiple small-aperture array sources (H_m) is greater than that of the magnetic field (H_s) excited by the single large-aperture loop so that we can define the relationship as below:

$$H_m = H_s + \Delta H \tag{1}$$

Table 1. Relative difference between secondary response to the copper plate object using the multi-aperture and single-aperture loop configurations

Buried depth (cm)	Relative difference
0	0.058
2	0.1532
4	0.165
6	0.318
8	0.257
10	0.224
12	0.19
14	0.147
16	0.138
18	0.126
20	0.108
22	0.098

where ΔH is the magnetic field difference. We have compared the differences between the multiple small-aperture sources and the single large-aperture source configurations for both the primary and the secondary fields with different offsets from the transmitter in the horizontal plane or buried depth in vertical extent. The results are summarised in Table 1.

We can see from Table 1 that the relative difference value generalised with two different systems mainly distributes around the range of 0.15–0.31. Based on the statistical data of Table 1, we can deduce the following equation

$$H_m^2 = H_s^2 + \Delta H_2 = H_s^2 + 31\% H_s^2 \tag{2}$$

The above relation indicates that the secondary field response can be improved by nearly 31% when switching from the single large-aperture loop to the multiple small-aperture array sources.

Case study

In order to construct a railway from Hubei province to Chongqing city, a series of tunnels have been designed. The tunnel for this case study is located in the south-west mountain area of Hubei province, in southwest China (see Figure 7). The test area is dominated by very complex geological conditions including tectonic denudation, erosion and corrosion of mountains. The altitude is approximately 400 m to 1400 m. The range of relative heights is 200 m to 1000 m.

The adopted geometry of the system is shown in Figure 8, where Figure 8*a* shows tunnel location. The length of the tunnel is 3.85 km. Figure 8*b* shows the configuration of the in-loop four-aperture TEM. During surveying, we adopted a configuration which fixed the transmitter loop and receiver antenna on a prop stand. A square transmitter loop (3 m × 3 m with 10 turns) was placed vertically on the front tunnel wall, and a small receiver coil (the antenna, see Figure 8*c*) with 210 m^2 in area was placed in the centre of the transmitter loop, with the antenna perpendicular to the plane of transmitter loop. This configuration was used to take soundings at numerous positions across the front wall of the tunnel. Data were recorded in the time delay range from 0.008 ms to 0.96 ms with a sampling frequency of 225 Hz. The output current was 10 A across a voltage of 24 V. The instrument, called terraTEM, was designed and built in Australia. Survey point intervals were 0.5 m.

We measured the parameter $V(t)/I$, where $V(t)$ denotes secondary induced voltage, I is sending current, and the units of $V(t)/I$ are $\mu V/A$. We convert $V(t)$ data into apparent resistivity data by:

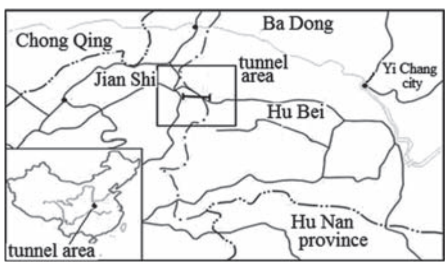

Fig. 7. *Location of the case study survey area.*

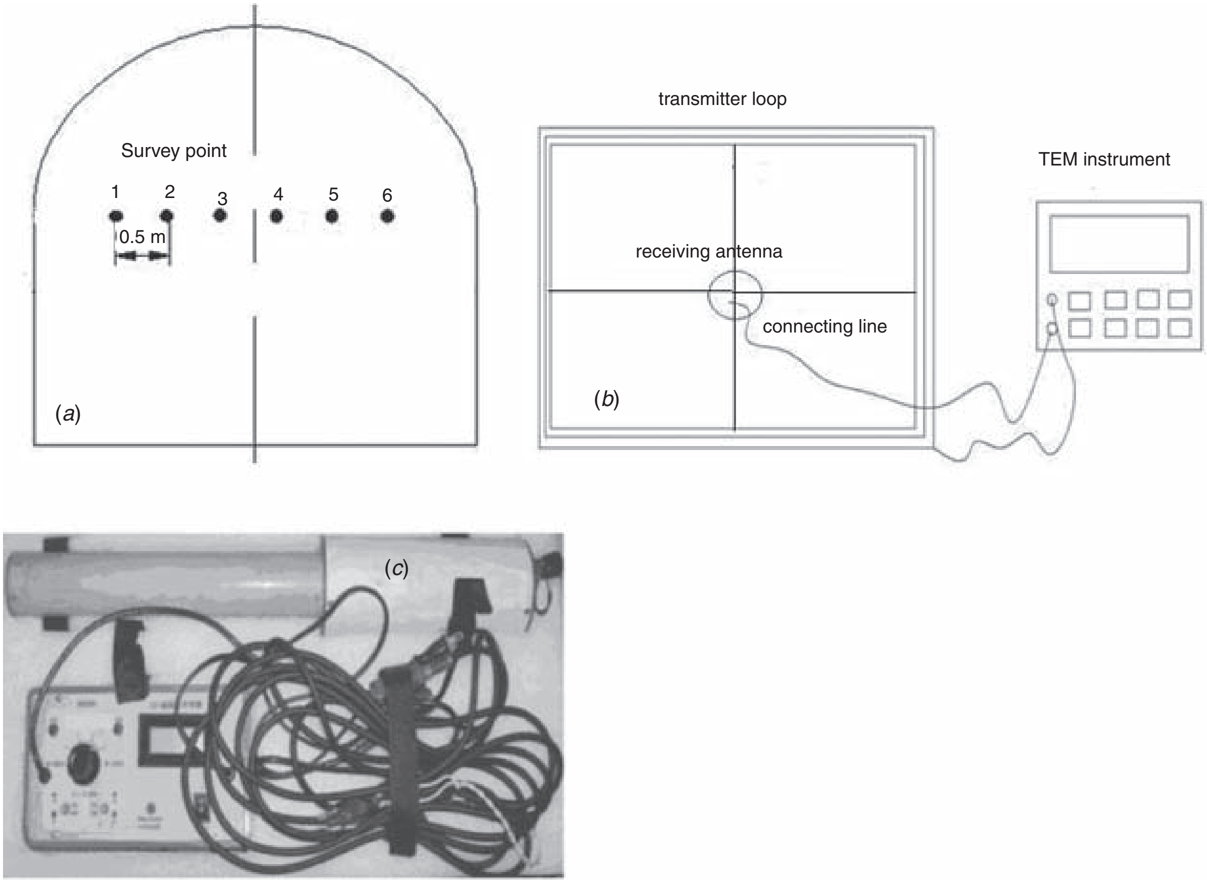

Fig. 8. *A sketch of the TEM configuration located at the surface of the tunnel.*

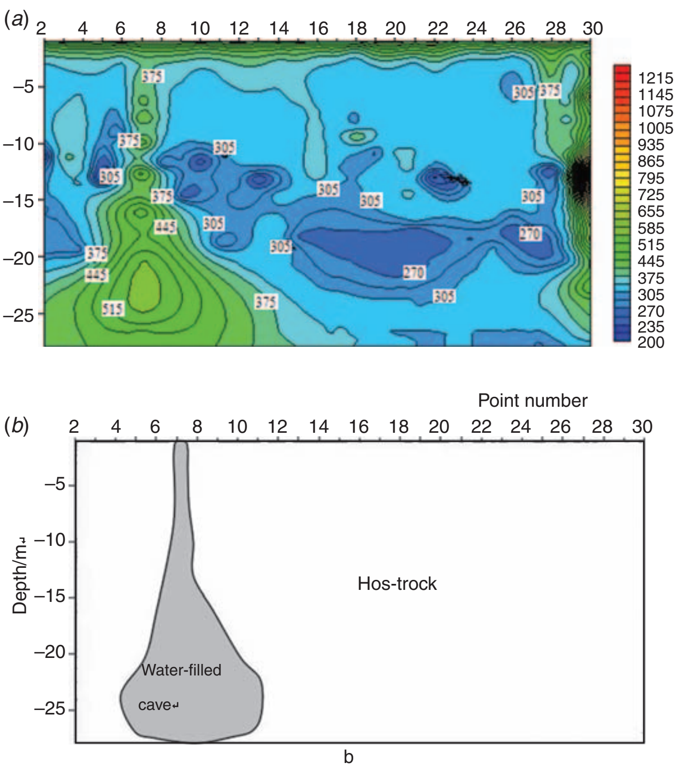

Fig. 9. *Example of interpreted tunnel data: (a) apparent resistivity contour; (b) the interpreted 2-D section and diagram.*

$$\rho(t) = \frac{\mu_0}{4\pi t}\left(\frac{2\mu_0 Mq}{5tV(t)}\right)^{2/3} \tag{3}$$

where M is the moment of transmitter, q is receiver area, and t is time delay.

We also transform prediction depth h_τ from $V(t)$ by

$$h_\tau = \left[\frac{3Mq}{16\pi V(t)\, S_t}\right]^{1/4} - \frac{t}{\pi_0 S_\tau} \tag{4}$$

$$\text{where } S_\tau = \frac{16\pi^{1/3}}{(3Mq)^{1/3}\mu_0^{4/3}} \frac{[V(t)]^{5/3}}{[V(t)]^{4/3}} \tag{5}$$

We calculated apparent resistivity and depth according to equations (3), (4) and (5).The results are shown in Figure 9, where Figure 9*a* shows apparent resistivity contours. The horizontal direction indicates the number of survey points, the interval spacing is 0.5 m, and vertical direction represents prediction depth, agreeing with the ex-cave direction. In the surface of the tunnel wall, the resistivity is high, which means that the rock stays well deposited. At survey point 7 and a depth of 25 m, there exists a low resistivity layer (displayed in green), which may be caused by a water filled structure. Figure 9*b* shows the final interpreted results based on available geological information. The interpreted results were tested by an ex-cave recorder during excavation. We found a large cave at a depth of 15 m corresponding to survey point 6. The height of this cave is 10 m and it appears to be a large-scale, full-water, full-mud feature.

Through the interpretation of transient electromagnetic data and comparing the calculated resistivity sections, we can infer the location and scope of a cave. After confirmation of the existence of this cave, we concluded that the transient electromagnetic interpretation was in agreement with the actual geological conditions.

Conclusion

TEM has been used extensively for surface exploration in China over the past few decades. However, there are few reports of TEM being applied in tunnel forecasting. We developed a specially designed TEM configuration, which can be used on a tunnel wall to detect water-filled structures.

The study demonstrates that employing a multi-aperture transmitter configuration can reform the direction of the scatter field, gather magnetic field of the scatter field to the centre of the transmitter loop, and as a result generate a high intensity of primary field in the centre of the loop. It suggests a bright future for the application of this theory and technology to improve the precision and resolution of TEM data. The result of the case study shows that the redesigned configuration can successfully be used to detect water or mud-filled faults or fracture zones ahead of the front wall of a tunnel during construction.

References

Christensen, N. B., and Sørensen, K. I., 1998, Surface and borehole electric and electromagnetic methods for hydrogeological investigations: *European Journal of Environmental and Engineering Geophysics* **3**, 75–90.

Dickmann, T., and Sander, B. K., 1996, Drivage concurrent Tunnel Seismic Prediction (TSP): *Felsbau* **14**(6), 406–411.

Raiche, A. P., Jupp, D. L. B., Rutter, H., and Vozoff, K., 1985, The joint use of coincident loop transient electromagnetic and Schlumberger sounding to resolve layered structure: *Geophysics* **50**, 1618–1627.

Spies, B. R., and Parker, P. D., 1984, Limitations of large-loop transient electromagnetic surveys in conductive terrains: *Geophysics* **49**, 902–912.

Strack, K. M., Lüschen, E., and Kötz, A. W., 1990, Long-offset transient electromagnetic (LOTEM) depth soundings applied to crustal studies in the Black Forest and Swabian Alb, Federal Republic of Germany: *Geophysics* **55**, 834–842.

Xue, G. Q., Song, J. P., and Yan, S., 2004, Detecting shallow caverns in China using TEM: *The Leading Edge* **23**(7), 694–695.

Zhang, Z., and Xiao, J., 2000, Inversions of surface and borehole data from large-loop transient electromagnetic system over a 1-D earth: *Geophysics* **66**, 1090–1096.

Zhdanov, M. S., 2006, Fast numerical modeling of multitransmitter electromagnetic data using multigrid quasi-linear approximation: *Geoscience & Remote Sensing, IEEE Transaction* **44**, 1428–1434.

Zhdanov, M. S., and Tartaras, E., 2002, Three-dimensional inversion of multitransmitter electromagnetic data based on the localized quasi-linear approximation: *Geophysical Journal International* **148**, 506–519.